Anchor Dependency for Non-Glycerol Based Cationic Lipofectins: Mixed Bag of Regular and Anomalous Transfection Profiles**

Rajkumar Sunil Singh,[a] Koushik Mukherjee,[a] Rajkumar Banerjee,[a] Arabinda Chaudhuri,*[a] Samik Kumar Hait,[b] Satya Priya Moulik,[b] Yerramsetti Ramadas,[c] Amash Vijayalakshmi,[c] and Nalam Madhusudhana Rao*[c]

Abstract: Although detailed structure–activity, physicochemical and biophysical investigations in probing the anchor influence in liposomal gene delivery have been reported for glycerol-based transfection lipids, the corresponding investigation for non-glycerol based simple monocationic transfection lipids have not yet been undertaken. Towards this end, herein, we delineate our structure–activity and physicochemical approach in deciphering the anchor dependency in liposomal gene delivery using fifteen new structural analogues (lipids **1**–**15**) of recently reported non-glycerol based monocationic transfection lipids. The C_{14} analogues in both series 1 (lipids **1**–**6**) and series 2 (lipids **7**–**15**) showed maximum efficiency in transfecting COS-1 and CHO cells. However, the C_{12} analogue of the ether series (lipid **3**) exhibited a seemingly anomalous behavior compared with its transfection efficient C_{10} and C_{14} analogues (lipids **2** and **4**) in being completely inefficient to transfect both COS-1 and CHO cells. The present structure–activity investigation also convincingly demonstrates that enhancement of transfection efficiencies through incorporation of membrane reorganizing unsaturation elements in the hydrophobic anchor of cationic lipids is not universal but cell dependent. The strength of the interaction of lipids **1**–**15** with DNA was assessed by their ability to exclude ethidium bromide bound to the DNA. Cationic lipids with long hydrophobic tails were found, in general, to be efficient in excluding EtBr from DNA. Gel to liquid crystalline transition temperatures of the lipids was measured by fluorescence anisotropy measurement technique. In general (lipid **2** being an exception), transfection efficient lipids were found to have their mid transition temperatures at or below physiological temperatures (37 °C).

Keywords: amphiphiles · lipids · liposomes · structure–activity relationships · transfection

Introduction

Use of efficient transfection vector is a prerequisite for success in gene therapy. The gene delivery efficiencies of viral vectors are, in general, superior to non-viral vectors. However, concern on the safety issues in using viral vectors are increasingly making the non-viral vectors as the alternative vector of choice. Among the several existing non-viral vectors,[1, 2] amphiphilic cationic transfection lipids[3–26] unquestionably hold promise in non-viral gene therapy. Robust manufacture, simplicity of handling techniques, least immunogenic response and ability to form stable injectable complexes even with large DNA are some of the distinct advantages associated with cationic transfection lipids.

Cationic transfection lipids are composed of three segments: a hydrophobic anchor, a linker and a head group. Efforts to delineate the contribution of each of these three segments on overall transfection efficiency is confounded by the complexity of the transfection pathway including formation of lipoplex along with the co-lipid, size and surface properties of the complexes, uptake and subsequent transport of the DNA into the nucleus. Different cell lines and plasmid constructs add to the complexity and make comparison of data obtained from different laboratories arduous.

[a] Dr. A. Chaudhuri, R. S. Singh, K. Mukherjee, R. Banerjee[+]
Division of Lipid Science and Technology
Indian Institute of Chemical Technology
Hyderabad 500 007 (India)
Fax: (+91) 40-7160757
E-mail: arabinda@iict.ap.nic.in

[b] S. K. Hait, S. P. Moulik
Centre for Surface Science, Department of Chemistry
Jadavpur University, Kolkata 700 032 (India)

[c] Dr. N. M. Rao, Y. Ramadas, A. Vijayalakshmi
Centre for Cellular and Molecular Biology
Hyderabad 500 007 (India)
Fax: (+91) 40-7171195
E-mail: madhu@ccmb.ap.nic.in

[+] Present Address: School of Pharmacy
University of Pittsburgh, Pennsylvania 19104 (USA)

[**] IICT Communication No. 4716.

0947-6539/02/0804-0900 $ 17.50+.50/0

Ever since Felgner et al.[26] pioneered the use of glycerol-backbone based cationic lipid (DOTMA) mediated gene delivery in 1987, intense global efforts have been witnessed for developing newer and more efficient cationic transfection lipids.[3–30] Interestingly, majority of the subsequently developed efficient cationic amphiphiles such as, DOTAP,[24] DMDHP,[10] DMRIE,[22] retained the glycerol backbone of DOTMA[26] (see Experimental Section for abbreviations) as the linker between the cationic head group and the hydrophobic tail region. Recently, we reported four remarkably efficient non-glycerol based nontoxic simple monocationic transfection lipids namely, DHDEAB, MOOHAC, DOMHAC and DOHEMAB,[5] in which the hydrophobic *n*-alkyl or *n*-alkenyl tails are covalently linked to the cationic head groups either directly or through an ester group. The most efficient one in this series is DHDEAB with two 2-hydroxyethyl head groups and two *n*-hexadecyl hydrophobic tails directly attached to the quaternary nitrogen atom. The transfection efficiency of DHDEAB is better than that of Lipofectamine, one of the most widely used commercial transfection agent.

Detailed structure – activity investigations in lipid mediated gene delivery using glycerol,[10, 22, 29, 30] polyamine[8, 9] and cholesterol[27, 28] based cationic transfection lipids with varying chain lengths hydrophobic tails, ether linker regions, unsaturated hydrophobic tails with membrane reorganizing capabilities have been reported. However, corresponding study using non-glycerol based cationic transfection lipids have not yet been undertaken. Towards this end, herein, with a view to probe the anchor-dependency profile in non-glycerol based cationic lipid mediated gene delivery, we have synthesized fifteen new (lipids **1**–**15**) structural analogues of our previously reported non-glycerol based highly efficient cationic transfection lipid DHDEAB.[5] The overall yields of the present DHDEAB structural analogues have been significantly improved in the new synthetic methods adopted in the present work. In the first series, to investigate the role of an additional ether linkage between the cationic head group and the hydrophobic anchor in modulating the transfection efficiencies of non-glycerol monocationic lipids, cationic amphiphiles **1**–**6** containing hydrophobic anchors with varying chain lengths linked to the quaternary nitrogen atom by an ether linkage were synthesized. In the second series, since membrane reorganizing ability of the lipoplex formulation is considered to be advantageous for transfection, chain lengths and unsaturation properties of the hydrophobic anchor in DHDEAB analogues were altered (amphiphiles **7**–**15**).

As delineated below, the C_{14} analogues in both series 1 (lipids **1**–**6**) and series 2 (lipids **7**–**15**) showed maximum efficiency in transfecting COS-1 and CHO cells. However, the C_{12} analogue of the ether series (lipid **3**) exhibited a seemingly anomalous behavior compared with its transfection efficient C_{10} and C_{14} analogues (lipids **2** and **4**) in being almost completely inefficient to transfect both COS-1 and CHO cells. The present structure – activity investigation also convincingly demonstrates that enhancement of transfection efficiencies through incorporation of membrane reorganizing unsaturation elements in the hydrophobic anchor of cationic lipids is not universal but cell dependent. The strength of the

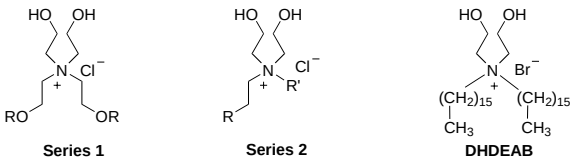

1: R = *n*-C_8H_{17}
2: R = *n*-$C_{10}H_{21}$
3: R = *n*-$C_{12}H_{25}$
4: R = *n*-$C_{14}H_{29}$
5: R = *n*-$C_{16}H_{33}$
6: R = *n*-$C_{18}H_{37}$

7: R' (= R-CH_2CH_2-) = *n*-C_8H_{17}
8: R' (= R-CH_2CH_2-) = *n*-$C_{10}H_{21}$
9: R' (= R-CH_2CH_2-) = *n*-$C_{12}H_{25}$
10: R' (= R-CH_2CH_2-) = *n*-$C_{14}H_{29}$
11: R' (= R-CH_2CH_2-) = *n*-$C_{16}H_{33}$
12: R' (= R-CH_2CH_2-) = *n*-$C_{18}H_{37}$
13: R' (= oleyl, R-CH_2CH_2-) = *n*-$C_{18}H_{35}$/*n*-$C_{18}H_{37}$
14: R' (= R-CH_2CH_2-) = oleyl
15: R' (= R-CH_2CH_2-) = *n*-$C_{20}H_{41}$

interaction of lipids **1**–**15** with DNA was assessed by their ability to exclude ethidium bromide bound to the DNA. Cationic lipids with long hydrophobic tails were found, in general, to be efficient in excluding EtBr from DNA. Gel to liquid crystalline transition temperatures of the lipids were measured by fluorescence anisotropy measurement technique. As outlined below, in general (lipid **2** being an exception), transfection efficient lipids were found to have their mid transition temperatures at or below physiological temperatures (37 °C).

Results and Discussion

Chemistry: The detailed synthetic procedures for the new cationic amphiphiles **1**–**6** with ether linkers and the new DHDEAB analogues **7**–**15** are outlined below in the Experimental Section. Amphiphiles **1**–**6** were synthesized by quaternizing the secondary amines containing the appropriate ether linkage (intermediate **V**, Scheme 1) with alkaline 2-chloroethanol. As outlined in Scheme 1, the necessary secondary amine intermediates **V** were synthesized by coupling the appropriate 2-aminoethyl *n*-alkyl ether (intermediate **IV**, Scheme 1) with the corresponding 2-bromoethyl-*n*-alkyl ether (intermediate **II**, Scheme 1) in presence of base. 2-Aminoethyl *n*-alkyl ether intermediates **IV** (Scheme 1) were conventionally synthesized from the 2-hydroxyethyl *n*-alkyl ether (**I**, Scheme 1) in three steps by converting the starting primary alcohol (**I**, Scheme 1) to the corresponding primary bromide (intermediate **II**), reaction of the primary bromide with sodium azide and finally reduction the resulting primary azides (intermediate **III**, Scheme 1).

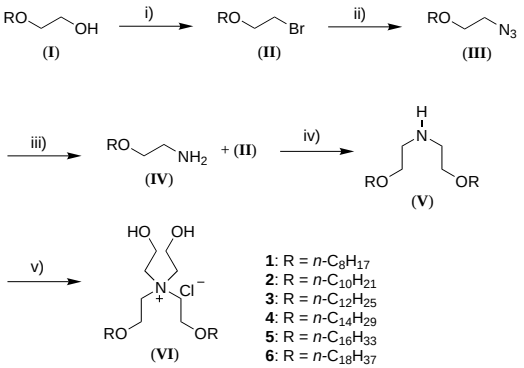

1: R = *n*-C_8H_{17}
2: R = *n*-$C_{10}H_{21}$
3: R = *n*-$C_{12}H_{25}$
4: R = *n*-$C_{14}H_{29}$
5: R = *n*-$C_{16}H_{33}$
6: R = *n*-$C_{18}H_{37}$

Scheme 1. Syntheses of new ether based cationic amphiphiles **1**–**6**. i) CBr_4, PPh_3, imidazole, dichloromethane; ii) NaN_3, dimethylformamide; iii) PPh_3, H_2O, tetrahydrofuran; iv) K_2CO_3/dimethylsulfoxide; v) excess chloroethanol, aqueous NaOH.

Much to our satisfaction, in the present work, we have succeeded in altering our previous low yield method[5] for synthesizing the DHDEAB analogues (lipids **7**–**15**). As outlined in Scheme 2, all the DHDEAB analogues were synthesized by quaternizing the hydrophobic secondary amine intermediates (**III**, Scheme 2) with 2-chloroethanol in presence of base. The necessary secondary amine intermediates (**III**, Scheme 2) were conventionally synthesized in two steps by coupling the primary amines (**I**) with the appropriate aldehydes (**II**, Scheme 2) followed by sodium borohydride reduction of the resulting imine.

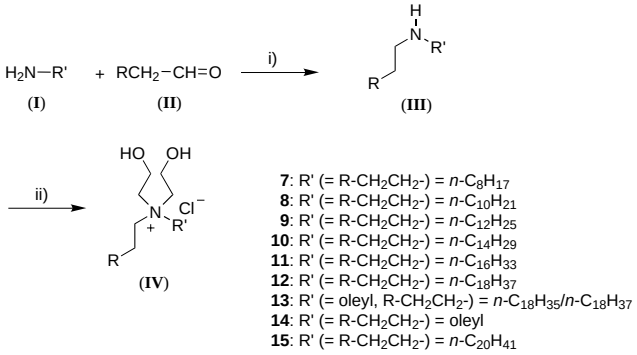

Scheme 2. Syntheses of new DHDEAB analogues. i) $MgSO_4$ (1 equiv), dichloromethane; ii) $NaBH_4$ (2 equiv), dichloromethane/MeOH; ii) excess chloroethanol/aqueous NaOH.

Transfection studies: To assess the transfection efficiencies of the amphiphiles **1**–**15**, we have used a plasmid containing β-galactosidase reporter gene under the control of a CMV promoter on two cell lines namely COS-1 (Figure 1) and CHO (Figure 2). Lipoplexes (containing 1:1 mol ratios of lipids and cholesterol) were prepared at charge ratios (+/−) ranging from 0.1 to 9.0 and tested for their transfection efficiency. Consistent with our previous observation,[5] the auxiliary lipid DOPE conventionally used in cationic liposome mediated gene delivery was found to be inefficient for the present DHDEAB structural analogues too (data not shown). Interestingly, without cholesterol as co-lipid, the present non-glycerol based lipids were found to be very poor in transfecting cells (as an representative example, the transfection data for lipids **4** and **10** both in presence and absence of cholesterol are shown in Figure 3). However, the exact role played by cholesterol in modulating the transfection efficiencies of the present transfection lipids is still an open question at this stage of investigation. In both COS-1 and CHO cells, C_{10} analogue of the ether based lipids (lipid **2**, series 1) showed its optimal transfection efficiency at lipid: DNA charge ratio of 0.3:1 whereas the equally efficient C_{14} analogue (lipid **4**, series 1) was most active at charge ratio (+/−) of 1:1 (Figures 1A and 2A). Surprisingly, the C_{12} analogue of the ether based lipid (lipid **3**, series 1) did not show any transfection activity in both COS-1 and CHO cells (Figures 1A and 2A).

Although lipids **1**–**6** (series 1) showed similar transfection activity profiles in both COS-1 and CHO cells (Figures 1A and 2A), lipids **7**–**15** (series 2) showed differential activity profiles in COS-1 and CHO cells (Figures 1B and 2B). In

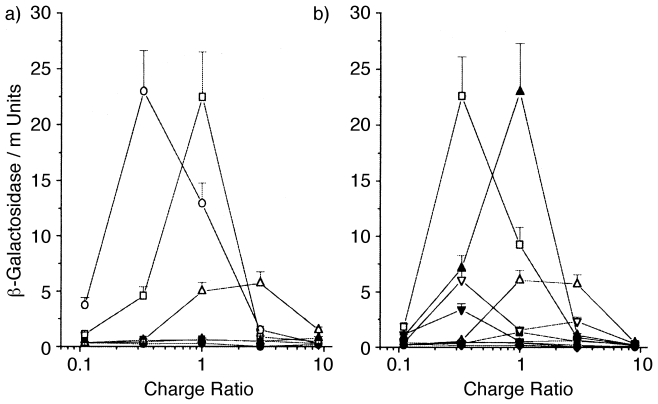

Figure 1. Transfection efficiencies of lipids **1**–**15** on COS-1 cells with cholesterol as co-lipid. a) Reporter gene activities of lipids **1**–**6** were plotted against charge ratios. **1** (●), **2** (○), **3** (■), **4** (□), **5** (▲) and **6** (△). b) Reporter gene activities of lipids **7**–**15** were plotted against charge ratios. **7** (●), **8** (○), **9** (■), **10** (□), **11** (▲), **12** (△), **13** (▼), **14** (▽) and **15** (◆). The β-galactosidase activities in each well (μmol of *ortho*-nitrophenol produced per hour) was converted to an absolute β-galactosidase milliunits using standard curve obtained with pure (commercial) β-galactosidase. The data shown are average values from four independent experiments ($n = 4$).

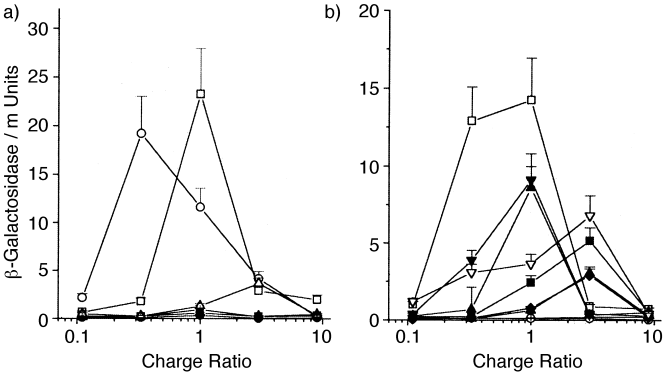

Figure 2. Transfection efficiencies of lipids **1**–**15** on CHO cells with cholesterol as co-lipid. a) Reporter gene activities of lipids **1**–**6** were plotted against charge ratio **1** (●), **2** (○), **3** (■), **4** (□), **5** (▲) and **6** (△). (B) Reporter gene activities of lipids **7**–**15** were plotted against charge ratios. **7** (●), **8** (○), **9** (■), **10** (□), **11** (▲), **12** (△), **13** (▼), **14** (▽)and **15** (◆).The β-galactosidase activities in each well (μmol of *ortho*-nitrophenol produced per hour) was converted to an absolute β-galactosidase milliunits using standard curve obtained with pure (commercial) β-galactosidase. The data shown are average values from four independent experiments ($n = 4$).

both COS-1 and CHO cells, the C_{14} analogue of DHDEAB[5] (lipid **10**, series 2) showed maximum transfection efficiency at lipid: DNA charge ratios 0.3:1 and 1:1, respectively (Figures 1B and 2B). However, the chloride counterion analogue of DHDEAB (lipid **11**, series 2) was about threefold more transfection efficient in COS-1 cells than in CHO cells at a +/− charge ratio of 1:1 (Figures 1B and 2B). Interestingly, lipids **13** and **14** (series 2) having one and two unsaturated double bonds, respectively, in the hydrophobic anchor were efficient in CHO cells (Figure 2B) while the transfection efficiencies of both were remarkably reduced in COS-1 cells (Figure 1B). This result convincingly indicates that the presence of membrane reorganizing unsaturation elements in the hydrophobic anchor of cationic lipids need not necessarily improve the transfection efficiency of cationic

0947-6539/02/0804-0902 $ 17.50+.50/0 *Chem. Eur. J.* **2002**, *8*, No. 4

amphiphiles, the effect is rather cell dependent in in vitro in liposomal gene delivery.

Transfection efficiencies of the present *non-glycerol* based monocationic lipids (lipids **4** and **10**) were observed to be higher than those of commercially available *glycerol based* monocationic transfection lipids such as, Lipofectin and DMRIE. Figure 3 shows a representative comparative data in COS-1 cells. Both lipids **10** and **4** were more than twofold and 3–4-fold transfection efficient than DMRIE and Lipofectin, respectively, in presence of cholesterol (not DOPE) as co-lipid (Figure 3). Pure lipids **10** and **4** (i.e., in absence of cholesterol) were found to be less efficient. The transfection efficiencies of lipids **4** and **10** were also observed to be higher than that of Lipofectamine, one of the most extensively used commercially available lipopolyamine based transfection lipids (Figure 3). However, the polycationic head group

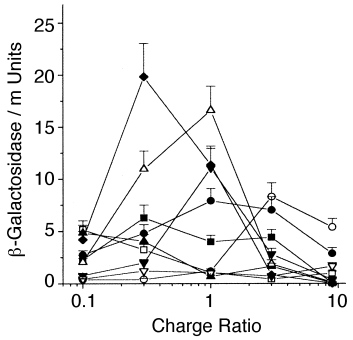

Figure 3. Comparison of the transfection efficiencies of lipid **4** and **10** with and without co-lipids (DOPE and cholesterol) on COS-1 cells. These efficiences were compared with DMRIE, Lipofectin and Lipofectamine. DMRIE (●), Lipofectamine (○), Lipofectin (■), pure lipid **4** (□), **4** with DOPE (▲), **4** with cholesterol (△), pure lipid **10** (▼), **10** with DOPE (▽) and **10** with cholesterol (◆).

nature of Lipofectamine (in contrast to monocationic head group of the present series) makes this latter comparison less relevant. Needless to say that the observed low cytotoxicities of the present lipids (shown below) and the higher in vitro transfection efficiencies of lipids **4** and **10** compared with Lipofectin and DMRIE justifies further in-depth structure–activity investigations using various new structural analogues of the present non-glycerol based transfection lipids. The outcome of such study is likely to add promising new non-glycerol based cationic amphiphiles to the arsenal of transfection lipids for future use in the area of non-viral gene therapy.

With a view to characterize the representative particle sizes, we have determined the particle sizes of the most transfection active lipoplexes made from lipids **4** and **10** using a dynamic light scattering spectrophotometer. Interestingly, the sizes of lipid **4**/DNA complexes were observed to be remarkably smaller than those of the lipid **10**/DNA lipoplexes (Table 1). Given similar transfection efficiences of lipids **4** and **10**, the lipoplex size data suggest that size does not have any correlation with the transfection efficiency. At this point of investigation, it is difficult to track the origin of such size difference. Whether or not, this remarkable size difference between the lipoplexes formed from lipids **4** and **10** will lead

Table 1. Particle sizes (the hydrodynamic diameter, d_h) of the representative liposomes and lipid/DNA complexes.

Lipid/DNA mol ratio	d_h[a] [nm]
lipid **4**	
1:0	43.4 ± 6.5
3:1	73.4 ± 11.0
1:1	89.5 ± 13.4
0.3:1	36.3 ± 5.45
lipid **10**	
1:0	229.3 ± 33.4
3:1	110.3 ± 16.5
1:1	258.8 ± 38.8
0.3:1	218.7 ± 32.8

[a] The DNA/lipid complexes were prepared by adding DNA to the liposomes at the charge ratios indicated. The particle sizes of pure liposomes and the lipid/DNA complexes were measured by a dynamic light scattering spectrophotometer. The concentrations of cationic lipids **4** and **10** and DNA used in size measurement experiments were same as those used in transfection experiments.

to any selective biodistributions and/or organ specific transgene expression in in vivo experiments needs to be investigated.

Toxicity studies: Cytotoxic effects of the lipoplexes made by the series 1 and 2 lipids were tested on COS-1 cell lines (Figure 4) using MTT assay.[32] The treatment protocols were identical for both cytotoxicity and transfection assays. Series 1 lipids are safer on the cells since, except for C_8 lipids, rest of the lipids have $<15\,\%$ loss in viability up to 3:1 charge ratio. In series 2, lipids with chain lengths less than C_{12} have maximal cytotoxic effect, whereas rest of the lipids have $<20\,\%$ loss of viability up to 3:1 charge ratio. Lipids in either series with shorter chain lengths may not form suitable complexes and may behave more as cell lysing detergents, hence their higher toxicity.

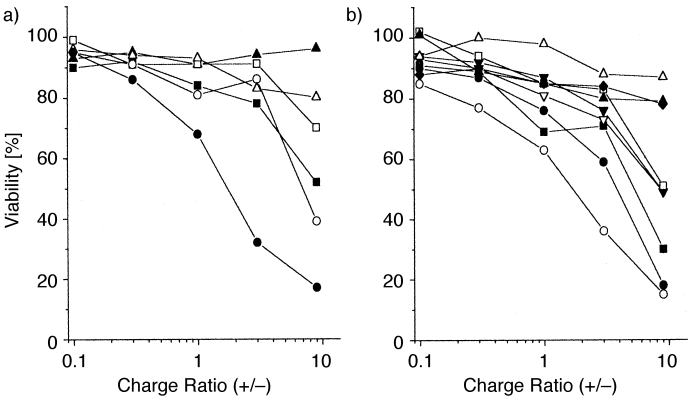

Figure 4. Cytotoxicity of lipids **1**–**15** on COS-1 cells. Toxicity, measured as percent viability, was plotted in a) **1** (●), **2** (○), **3** (■), **4** (□), **5** (△) and **6** (▲) and in b) **7** (●), **8** (○), **9** (■), **10** (□), **11** (▲), **12** (△), **13** (▽), **14** (▼) and **15** (◆). The absorption obtained using reduced formazon with cells in the absence of lipids was taken to be 100. Results were expressed as per cent viability = $[A_{540}(\text{treated cells}) - \text{background}]/[A_{540}(\text{untreated cells}) - \text{background}] \times 100$.

DNA–lipid interactions probed by ethidium bromide binding: The strength of the interaction of lipids **1**–**15** with DNA was assessed by their ability to exclude ethidium bromide

(EtBr) bound to the DNA. Detail titration curves of all fifteen lipids with plasmid DNA indicated that ability of a lipid to interact with the DNA and to exclude EtBr was strongly dependent on the anchor chain length (Figure 5). Cationic lipids with long hydrophobic tails were found, in general, to be efficient in excluding EtBr from DNA. Results shown in Figure 5 also demonstrate that the EtBr displacement efficiencies of lipids **3** and **4** in series 1 are remarkably comparable to those of lipids **9**, **10** and **11** of series 2. Similarly, lipids **5** and **6** in series 1 and lipids **14** and **15** of series 2 exhibited comparable EtBr displacement (Figure 5). Given that additional -C–C–O- linkage present in the molecular architectures of lipids **1**–**6** in series 1 increases their effective anchor lengths, these results are consistent with anchor chain length dependent EtBr displacement. However, among all the lipids **1**–**15** studied in the present work, lipids **12** and **13** of series 2 turned out to be the most efficient in displacing EtBr from DNA (Figure 5). Thus, in general, presence of saturated hydrocarbon chain anchors containing 18 or less carbon atoms significantly enhances the lipid/DNA interactions for non-glycerol based monocationic transfection lipids containing dihydroxyethyl head groups.

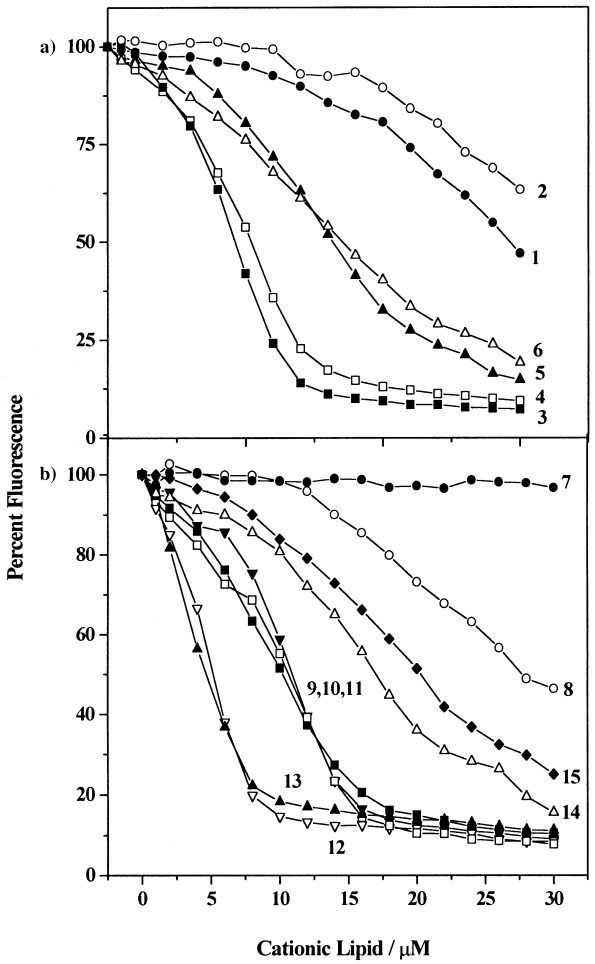

Figure 5. DNA and lipid interaction assessed by exclusion of ethidium bromide from DNA: Exclusion of ethidium bromide, monitored as decrease in fluorescence was plotted against the various charge raios of lipids **1**–**6** (a) and **7**–**15** (b). The order of addition of ethidium bromide or cationic lipids did not alter the final equilibrium fluorescence value.

Anisotropy measurements: Membrane fluidity of the cationic liposomes is known to be an advantage in transfection. Fluid membranes may assist fusion of lipoplexes with the endosomes and release the DNA into the cytoplasm efficiently. With a view to probe the role of membrane fluidity in modulating the transfection efficiencies, we studied the gel to liquid crystalline transition temperature of lipids **2**–**6** and **9**–**15** by fluorescence anisotropy measurement technique using DPH as fluorescent probe. Lipids **1**, **7** and **8** did not entrap any DPH to take anisotropy measurements. The shorter chain lengths of these lipids probably did not allow them to make vesicles. This is also corroborated by their poor interactions with DNA (Figure 5). The mid-points of transition for lipids **4**, **5** and **6** in series 1 were observed to be 23 °C, 38 °C and 50 °C, respectively (Figure 6A). Such increase in transition temperatures was consistent with the increasing anchor chain lengths for lipids **4**–**6** in series 1. Lipids **2** and **3** did not show any transition in the observed temperature range but their high anisotropy values indicate that the membrane of these vesicles is rigid. Lipids **11**, **12** and **15** of series 2 showed transition temperature with mid-point of transition being 22 °C, 52 °C and 53 °C, respectively (Figure 6B). The mid-point of transition of series 2 lipids were also observed to increase with their chain length. Lipids **9**–**10** and **13**–**14** did not show any transition and all of them have low anisotropy values (Figure 6B) indicating the fluid nature of the liposome membranes made from these lipids across the temperature range tested. Given that -CH_2–CH_2–O- spacer for series 1 lipids are part of their hydrophobic tails, the anchor lengths of lipids **2** and **9** are likely to be close. However, the fluorescence anisotropy in liposomes made with lipid **2** was found to be significantly higher than that of lipid **9** (Figure 6A and B). Similarly, inspite of having similar anchor lengths, the observed fluorescence anisotropy of liposomes made with lipid **3** was remarkably higher than that of liposome made from lipid **10** (Figure 6). Such unexpectedly higher membrane anisotropy associated with lipids **2** and **3** indicate that the ether link in lipids **2** and **3** may be involved in additional interactions to rigidify their liposomal membrane. Unsaturated hydrophobic chains present in lipids **13** and **14** increased the membrane fluidity as expected.

When compared with the transfection efficiency, lipids that have transition temperatures at or below physiological temperatures (37 °C) are efficient. Lipid **2** was an exception with mid-point of transition well above 37 °C though based on chain length should have transition temperature below 37 °C. Probably head-group interactions come to the fore in this lipid. Our results are comparable to similar study with analogues of DOTAP[29] in which myristoyl derivatives were shown to have higher transfection efficiency than lauroyl, palmitoyl, stearoyl or oleoyl derivatives of DOTAP using cholesterol as co-lipid. Only myristoyl derivative of DOTAP alone had mid-point of transition near 37 °C. Our studies demonstrate that unsaturated chains do not impart any transfection advantage compared with the saturated chains (Figure 2). Liposomes in solid gel-like phase would be less flexible in their interaction with the DNA or with the cell membranes. Interestingly, liposomes made from lipid **3** did not exhibit any well defined mid-point of temperature of

0947-6539/02/0804-0904 $ 17.50+.50/0 *Chem. Eur. J.* **2002**, *8*, No. 4

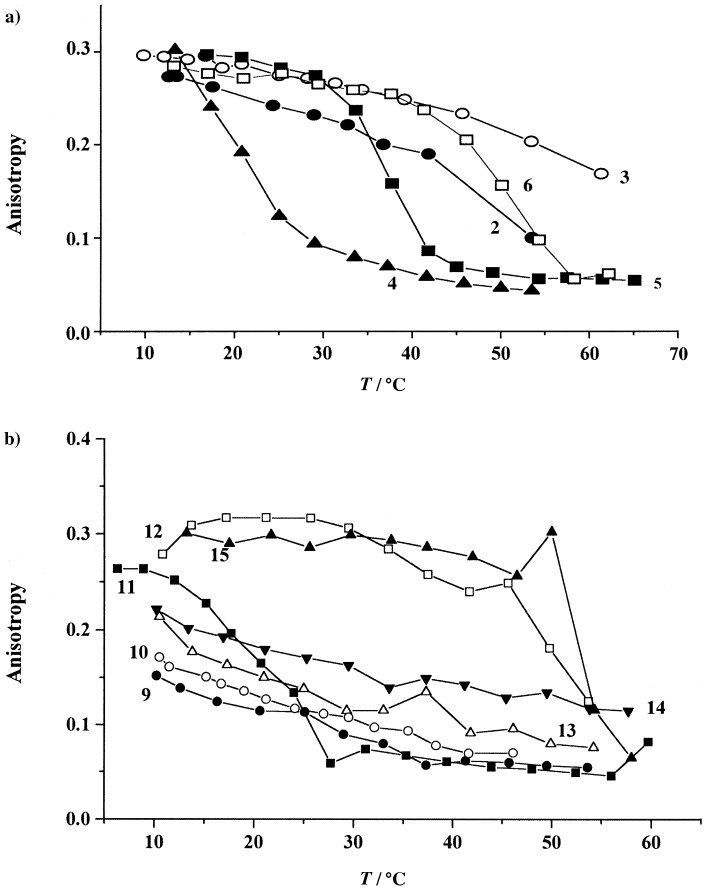

Figure 6. Temperature dependent anisotropy measurements of lipids **2**–**6** and **9**–**15**: Parallel and perpendicular fluorescence of pure cationic lipid vesicles preloaded with DPH was recorded at various temperatures. Anisotropy was calculated as described in the Experimental Section for lipids **2**–**6** (a) and lipids **9**–**15** (a). Lipids **1**, **7** and **8** did not entrap any DPH to take anisotropy measurements. Temperature in the cuvette was measured with a precalibrated thermocouple.

transition within the experimental temperature range 10°–65°C (Figure 6) indicating the possible existence of a solid gel-like membrane for these liposomes. It can not be determined from the present data whether or not the complete lack of transfection observed for lipid **3** in both COS-1 and CHO cell lines (Figures 1 and 2) has its origin to high membrane rigidity associated with liposomes prepared using lipid **3**.

Conclusion

In summary, the present investigation outlines structure–activity and physicochemical approach in deciphering the anchor-dependency profile in in vitro liposomal gene delivery using fifteen new structural analogues (lipids **1**–**15**) of our recently reported efficient non-glycerol based cationic transfection lipid DHDEAB.[5] Present investigation demonstrate that quaternization of hydrophobic secondary amines containing the desired alkyl/alkenyl chains with alkaline 2-chloroethanol is a very simple route for synthesizing non-glycerol based transfection efficient DHDEAB-structural analogues. The C_{14} analogues in both series 1 (lipids **1**–**6**) and series 2 (lipids **7**–**15**) showed maximum efficiency in transfecting COS-1 and CHO cells. However, the C_{12} analogue of the ether series (lipid **3**) exhibited a seemingly anomalous behavior compared to its transfection efficient C_{10} and C_{14} analogues (lipids **2** and **4**) in being completely inefficient to transfect both COS-1 and CHO cells. Myristyl anchor containing lipids were found to be optimal both in interacting with DNA and in their transfection efficiency. The present structure–activity investigation convincingly demonstrates that enhancement of transfection efficiencies through incorporation of membrane reorganizing unsaturation elements in the hydrophobic anchor of cationic lipids is not universal but cell dependent. Cationic lipids with long hydrophobic tails were found, in general, to be efficient in excluding EtBr from DNA. In general (lipid **2** being an exception), transfection efficient lipids were found to have their mid transition temperatures at or below physiological temperatures (37°C). Lipids **10** and **4**, being more than twofold and 3–4-fold transfection efficient than DMRIE and Lipofectin, respectively, are two new promising cationic transfection lipids for future use in the area of non-viral gene delivery.

Experimental Section

Abbreviations: DHDEAB: *N*,*N*-di-*n*-hexadecyl-*N*,*N*-dihydroxyethylammonium bromide; DMDHP: (±)-*N*,*N*-[Bis(2-hydroxyethyl)]-*n*-[2,3-bis-(tetradecanoyloxy)propyl]ammonium chloride; DMRIE: 1,2-dimyristyloxypropyl-3-dimethyl-hydroethyl ammonium bromide; DOTAP: 1,2-dioleoyloxy-3-(trimethylamino)propane; DOTMA: 1,2-dioleyl-3-*N*,*N*,*N*-trimethylaminopropane chloride; DOPE: 1,2-dioleoyl-propyl-3-phosphatidylethanolamine.

General procedures and materials: The high-resolution mass spectrometric (HRMS) analysis were performed on a Micromass AUTOSPEC-M mass spectrometer (Manchester, UK) with OPUS V3.1X data system. Data were acquired by liquid secondary ion mass spectrometry (LSIMS) technique using *meta*-nitrobenzyl alcohol as the matrix. LSIMS analysis were performed in the scan range 100–1000 amu at the rate of 3 scans s^{-1}. ^{1}H NMR spectra were recorded on a Varian FT 200 MHz or Varian Unity 400 MHz. 1-Bromooctane, 1-bromodecane, 1-bromododecane, 1-bromotetradecane, 1-bromohexadecane, 1-bromooctadecane, sodium hydride, sodium borohydride and carbon tetrabromide were purchased from Lancaster (Morecambe, England). Unless otherwise stated, all reagents were purchased from local commercial suppliers and were used without further purification. Column chromatography was performed with silica gel (Acme Synthetic Chemicals, India, finer than 200 and 60–120 mesh). pCMV.SPORT-β-gal, Lipofectamine, cell culture media and fetal calf serum were purchased from GibcoBRL, Rockville, USA. 3-(4,5-Dimethylthiazol-2-yl)-2,5-diphenyltetrazolium bromide (MTT), polyethylene glycol 8000, NP-40, antibiotics, agarose, *o*-nitrophenyl-β-D-galactopyranoside were purchased from Sigma, St. Louis, USA. DNA molecular weight markers were purchased from Bangalore Genei, Bangalore, India. Cholesterol and dioleoyl phosphatidyl ethanolamine (DOPE) were purchased from Avanti Polar, Alabama, USA. COS-1 cell line (SV 40 transformed African green monkey kidney, ATCCCRL 1650) and CHO (chinese hamster ovary) was obtained from ATCC, Maryland, USA. Unless otherwise stated, all reagents were purchased from local commercial suppliers and were used without further purification.

Syntheses

All the 2-haloethyl *n*-alkyl ether starting materials used to synthesize the cationic amphiphiles **1**–**6** were prepared following the same protocol outlined in Scheme 1. As a representative example, synthesis of 2-bromoethyl *n*-dodecyl ether is described below in detail.

2-Bromoethyl *n*-dodecyl ether: 2-Hydroxyethyl *n*-dodecyl ether (1 g, 4.34 mmol, prepared conventionally by reacting 1-bromododecane with

ethylene glycol and NaH at 80 °C in dry dimethylformamide under N_2 for 2–3 d), triphenylphosphine (2.28 g, 8.69 mmol) and imidazole (591.4 mg, 8.69 mmol) were dissolved in a 50 mL two-necked round-bottomed flask in dry dichloromethane (3 mL) under nitrogen atmosphere. The solution was cooled to 0 °C, carbon tetrabromide (2.88 g, 8.69 mmol, dissolved in 2 mL dry dichloromethane) was added dropwise to the cold solution and the temperature of the reaction mixture was gradually (1 h) raised to room temperature. The reaction mixture was then stirred for 20 h at room temperature, concentrated and column chromatographic purification (using 60–120 mesh size silica gel and 5–7% ethyl acetate in hexane as the eluent) of the residue afforded the pure title compound as a colorless liquid (800 mg, 78.5%). $R_f = 0.50$ (hexane/ethyl acetate 95:5). ^{1}H NMR (200 MHz, $CDCl_3$): $\delta = 0.90$ [t, 3H, CH_3-$(CH_2)_9$-], 1.20–1.42 [m, 18H, -$(CH_2)_9$-], 1.50–1.65 [m, 2H, Br-CH_2-CH_2-O-CH_2-CH_2-$(CH_2)_8$-], 3.35–3.50 [m, 4H, Br-CH_2-CH_2-O-CH_2-], 3.70 [t, 2H, Br-CH_2-CH_2-O-].

2-Bromoethyl *n*-octyl ether: ^{1}H NMR (200 MHz, $CDCl_3$): $\delta = 0.90$[t, 3H, CH_3-$(CH_2)_5$-], 1.20–1.40 [m, 10H, -$(CH_2)_5$-], 1.50–1.65 [m, 2H, Br-CH_2-CH_2-O-CH_2-CH_2-], 3.35–3.50 [m, 4H, Br-CH_2-CH_2-O-CH_2-], 3.70 [t, 2H, Br-CH_2-CH_2-O-].

2-Bromoethyl *n*-decyl ether: ^{1}H NMR (200 MHz, $CDCl_3$): $\delta = 0.88$ [t, 3H, CH_3-$(CH_2)_7$-], 1.15–1.40 [m, 14H, -$(CH_2)_7$-], 1.50–1.65 [m, Br-CH_2-CH_2-O-CH_2-CH_2-], 3.35–3.50 [m, 4H, Br-CH_2-CH_2-O-CH_2-], 3.70 [t, 2H, Br-CH_2-CH_2-O-].

2-Bromoethyl *n*-tetradecyl ether: ^{1}H NMR (200 MHz, $CDCl_3$): $\delta = 0.90$ [t, 3H, CH_3-$(CH_2)_{11}$-], 1.20–1.40 [22H, -$(CH_2)_{11}$-], 1.57 [q, 2H, -O-CH_2-CH_2-$(CH_2)_{11}$-], 3.37–3.50 [m, 4H, Br-CH_2-CH_2-O-CH_2-], 3.70 [t, 2H, Br-CH_2-CH_2-O-].

2-Bromoethyl *n*-hexadecyl ether: ^{1}H NMR (200 MHz, $CDCl_3$): $\delta = 0.90$ [t, 3H, CH_3-$(CH_2)_{11}$-], 1.18–1.40 [m, 26H, -$(CH_2)_{13}$-], 1.50–1.62 [m, 2H, -O-CH_2-CH_2-$(CH_2)_{11}$-], 3.38–3.50 [m, 4H, Br-CH_2-CH_2-O-CH_2-], 3.70 [t, 2H, Br-CH_2-CH_2-O-].

2-Chloroethyl *n*-octadecyl ether: ^{1}H NMR (200 MHz, $CDCl_3$): $\delta = 0.90$ [t, 3H, CH_3-$(CH_2)_{15}$-], 1.15–1.40 [m, 30H, -$(CH_2)_{15}$-], 3.47 [t, 2H, Cl-CH_2-CH_2-O-CH_2-], 3.55–3.70 [m, 4H, Cl-CH_2-CH_2-O-].

All the 2-azidoethyl-*n*-alkyl ether intermediates used to synthesize cationic amphiphiles **1–6** were prepared following the same protocol outlined in Scheme 1. As a representative example, synthesis of 2-azidoethyl-*n*-dodecyl ether is described below in detail.

Synthesis of 2-azidoethyl *n*-dodecyl ether: In a 15 mL round-bottomed flask, NaN_3 (443.3 mg, 6.82 mmol) was added to 2-bromoethyl *n*-dodecyl ether (400 mg, 1.36 mmol) dissolved in dry dimethylformamide (2 mL) under nitrogen and the temperature of the reaction was raised to 60 °C. The reaction mixture was kept under stirring at 60 °C for 16 h. The temperature of the reaction mixture was gradually lowered to room temperature, water (15 mL) added and the reaction mixture extracted with ethyl acetate (3 × 20 mL). The organic phases were then washed with saturated brine solution (3 × 15 mL), dried with anhydrous Na_2SO_4, filtered and the filtrate was concentrated on a rotary evaporator. Column chromatographic (using 60–120 mesh size silica and 5–7% (*v*/*v*) ethyl acetate in hexane as eluent) of the residue afforded the pure title compound as a colorless liquid (345 mg, 99%). $R_f = 0.40$ (hexane/ethyl acetate 95:5). ^{1}H NMR (200 MHz, $CDCl_3$): $\delta = 0.90$ [t, 3H, CH_3-$(CH_2)_9$-], 1.15–1.40 [m, 18H, -$(CH_2)_9$-], 1.50–1.65 [m, -O-CH_2-CH_2-CH_2-], 3.32 [t, 2H, N_3-CH_2-CH_2-O-CH_2-], 3.42 [t, 2H, N_3-CH_2-CH_2-], 3.55 [t, 2H, N_3-CH_2-CH_2-O-].

2-Azidoethyl octyl ether: ^{1}H NMR (200 MHz, $CDCl_3$): $\delta = 0.90$ [t, 3H, CH_3-$(CH_2)_5$-], 1.15–1.45 [m, 10H, -(CH_2)-], 1.50–1.65 [m, 2H, -O-CH_2-CH_2-CH_2-], 3.35 [t, 2H, N_3-CH_2-CH_2-O-CH_2-], 3.45 [t, 2H, N_3-CH_2-CH_2-O-], 3.60 [t, 2H, N_3-CH_2-CH_2-O-].

2-Azidoethyl decyl ether: ^{1}H NMR (200 MHz, $CDCl_3$): $\delta = 0.90$ [t, 3H, CH_3-$(CH_2)_7$-], 1.20–1.50 [m, 14H, -$(CH_2)_7$], 1.50–1.70 [m, 2H, -O-CH_2-CH_2-CH_2-], 3.35 [t, 2H, N_3-CH_2-CH_2-O-CH_2-], 3.45 [t, 2H, N_3-CH_2-CH_2-O-], 3.60 [t, 2H, N_3-CH_2-CH_2-O-].

2-Azidoethyl tetradecyl ether: ^{1}H NMR (200 MHz, $CDCl_3$): $\delta = 0.90$ [t, 3H, CH_3-$(CH_2)_{11}$-], 1.15–1.40 [m, 22H, -$(CH_2)_{11}$-], 1.50–1.62 [m, 2H, -O-CH_2-CH_2-CH_2-], 3.32 [t, 2H, N_3-CH_2-CH_2-O-CH_2-], 3.45 [t, 2H, N_3-CH_2-CH_2-O-], 3.58 [t, 2H, N_3-CH_2-CH_2-O-].

2-Azidoethyl hexadecyl ether: ^{1}H NMR (200 MHz, $CDCl_3$): $\delta = 0.90$ [t, 3H, CH_3-$(CH_2)_{13}$-], 1.201.40 [m, 26H, -$(CH_2)_{13}$-], 1.50–1.65 [m, 2H, -O-CH_2-CH_2-CH_2-], 3.35 [t, 2H, N_3-CH_2-CH_2-O-CH_2-], 3.45 [t, 2H, N_3-CH_2-CH_2-O-], 3.60 [t, 2H, N_3-CH_2-CH_2-O-].

2-Azidoethyl octadecyl ether: ^{1}H NMR (200 MHz, $CDCl_3$): $\delta = 0.90$ [t, 3H, CH_3-$(CH_2)_{15}$-], 1.15–1.40 [m, 30H, -$(CH_2)_{15}$-], 1.50–1.65 [m, 2H, -O-CH_2-CH_2-CH_2-], 3.35 [t, 2H, N_3-CH_2-CH_2-O-CH_2-], 3.45 [t, 2H, N_3-CH_2-CH_2-O-], 3.60 [t, 2H, N_3-CH_2-CH_2-O-].

All the 2-aminoethyl *n*-alkyl ether intermediates used to synthesize the cationic amphiphiles **1–6** were prepared following the same protocol outlined in Scheme 1. As a representative example, synthesis of 2-aminoethyl-*n*-dodecyl ether is described below in detail.

2-Aminoethyl *n*-dodecyl ether: In a 25 mL round-bottomed flask, a mixture of 2-azidoethyl *n*-dodecyl ether (330 mg, 1.29 mmol) and triphenyl phosphine (508.7 mg, 1.94 mmol) dissolved in tetrahydrofuran (2 mL) was stirred at room temperature. Effervescence was observed. After 10 min, water (three drops) was added and the reaction mixture was kept under stirring for 38 h. The reaction mixture was then concentrated on a rotary evaporator and column chromatographic purification of the residue (using 60–120 mesh size silica and 5–10% methanol in chloroform as the eluent) afforded the pure title compound (280.5 mg, 94.6%) as a pale yellow colored liquid. $R_f = 0.30$ (chloroform/methanol 90:10); ^{1}H NMR (200 MHz, $CDCl_3$): $\delta = 0.90$ [t, 3H, CH_3-$(CH_2)_9$-], 1.15–1.40 [m, 18H, -$(CH_2)_9$-], 1.50–1.65 [m, 2H, -O-CH_2-CH_2-CH_2-], 2.90 [t, 2H, NH_2-CH_2-CH_2-], 3.35–3.55 [m, 4H, -CH_2-O-CH_2-], 3.60 [brs, 2H, NH_2-].

2-Aminoethyl *n*-octyl ether: ^{1}H NMR (200 MHz, $CDCl_3$): $\delta = 0.88$ [t, 3H, CH_3-$(CH_2)_5$-], 1.15–1.40 [m, 10H, -$(CH_2)_5$-], 1.45–1.62 [m, 2H, -O-CH_2-CH_2-CH_2-], 3.00 [m, 2H, NH_2-CH_2-CH_2-]; 3.45 [t, 2H, NH_2-CH_2-CH_2-O-CH_2-], 3.55 [t, 3H, NH_2-CH_2-CH_2-O-], 4.68 [brs, 2H, NH_2-].

2-Aminoethyl *n*-decyl ether: ^{1}H NMR (200 MHz, $CDCl_3$): $\delta = 0.88$ [t, 3H, CH_3-$(CH_2)_7$-], 1.15–1.40 [m, 14H, -$(CH_2)_7$-], 1.45–1.60 [m, 2H, -O-CH_2-CH_2-CH_2-], 2.87 [t, 2H, NH_2-CH_2-CH_2-], 3.00 [brs, 2H, NH_2-], 3.33–3.45 [m, 4H, -CH_2-O-CH_2-].

2-Aminoethyl *n*-tetradecyl ether: ^{1}H NMR (200 MHz, $CDCl_3$): $\delta = 0.90$ [t, 3H, CH_3-$(CH_2)_{11}$-], 1.15–1.40 [m, 22H, -$(CH_2)_{11}$-], 1.45–1.60 [m, -O-CH_2-CH_2-CH_2-], 2.90 [brs, 2H, NH_2-CH_2-CH_2-], 3.35–3.50 [m, 4H, -CH_2-O-CH_2-], 3.55 [brs, 2H, NH_2-].

2-Aminoethyl *n*-hexadecyl ether: ^{1}H NMR (400 MHz, $CDCl_3$): $\delta = 0.88$ [t, 3H, CH_3-$(CH_2)_{13}$-], 1.20–1.40 [m, 26H, -$(CH_2)_{13}$-], 1.50–1.62 [m, 2H, -O-CH_2-CH_2-CH_2-], 2.83 [t, 2H, NH_2-CH_2-CH_2-O-], 3.38–3.45 [m, 4H, -CH_2-O-CH_2-].

2-Aminoethyl *n*-octadecyl ether: ^{1}H NMR (200 MHz, $CDCl_3$): $\delta = 0.90$ [t, 3H, CH_3-$(CH_2)_{15}$-], 1.15–1.40 [m, 30H, -$(CH_2)_{15}$-], 1.50–1.65 [m, 2H, -O-CH_2-CH_2-CH_2-], 2.97 [t, 2H, NH_2-CH_2-CH_2-O-], 3.10 [brs, NH_2-CH_2-], 3.42–3.57 [m, 4H, -CH_2-O-CH_2-].

The secondary amine intermediates (**IV**, Scheme 1) in the syntheses of amphiphiles **1–6** were not isolated as pure compounds. Instead, the crude secondary amines were subjected to quaternization with alkaline 2-chloroethanol. As a representative example, synthetic details for *N*,*N*-di-[2-*n*-dodecyloxyethyl]-*N*,*N*-di-[2-hydroxyethyl]ammonium chloride (amphiphile **3**, Scheme 1) is outlined below.

***N*,*N*-Di-[2-*n*-dodecyloxyethyl]-*N*,*N*-di-[2-hydroxyethyl]ammonium chloride (3, Scheme 1)**: In a 10 mL round-bottomed flask, a mixture of 2-aminoethyl *n*-dodecyl ether (240 mg, 1.05 mmol), 2-bromoethyl *n*-dodecyl ether (307 mg, 1.05 mmol), and potassium carbonate (173.3 mg, 1.26 mmol) were taken in dimethyl sulfoxide (1 mL) and the reaction mixture was heated to 65 °C. The reaction mixture was kept under stirring for 42 h. Saturated brine solution (15 mL) was added to the reaction mixture and extracted with ethyl acetate (3 × 20 mL). The combined organic phases was dried with anhydrous Na_2SO_4, filtered and the filtrate was concentrated on a rotary evaporator. The secondary amine intermediate, *N*,*N*-di-[2-*n*-dodecyloxyethyl]amine (**IV**, Scheme 1) was purified further from the residue by silica gel column chromatography using 60–120 mesh size silica and 4% methanol in chloroform (*v*/*v*) as the eluent. The combined fractions eluted with 4% methanol in chloroform was concentrated and the residue (401 mg, pale yellow semisolid) was quaternized using 2-chloroethanol and NaOH as described below.

A mixture of the residue obtained above (155 mg), chloroethanol (2 mL) and NaOH (150 mg in 0.5 mL water) in a 5 mL round-bottomed flask was stirred at 110 °C for 38 h. The unreacted 2-chloroethanol was evaporated from the reaction mixture as far as possible by raising the temperature to

0947-6539/02/0804-0906 $ 17.50+.50/0 *Chem. Eur. J.* **2002**, *8*, No. 4

130 °C. The residual 2-chloroethanol was removed on a rotary evaporator by repeated addition of methanol. Column chromatographic purification of the resulting residue using 60–120 mesh size silica and 8–10% methanolic chloroform (*v*/*v*) as the eluent afforded pure title cationic amphiphile (**V**, Scheme 1) as a colorless semi solid (98.4 mg, 49.4%). $R_f = 0.30$ (chloroform/methanol 90:10).

***N,N*-Di-[2-*n*-dodecyloxyethyl]-*N,N*-di-[2-hydroxyethyl]ammonium chloride (3)**: ^{1}H NMR (200 MHz, $CDCl_3$): $\delta = 0.90$ [t, 6H, CH_3-$(CH_2)_9$-], 1.20–1.45 [m, 36H, -$(CH_2)_9$-], 1.45–1.60 [m, 4H, -O-CH_2-CH_2-$(CH_2)_9$-], 3.45 [t, 4H, -O-CH_2-$(CH_2)_{10}$-], 3.70–3.95 [m, 12H, (HO-CH_2-$CH_2)_2N^+$(CH_2-CH_2-O-)$_2$-], 4.05–4.15 [m, 4H, (HO-CH_2-$CH_2)_2N^+$(CH_2-CH_2-O-)$_2$]; HRMS (LSIMS): *m*/*z*: calcd for $C_{32}H_{68}NO_4$: 530.5148; found: 530.5160.

***N,N*-Di-[2-*n*-octyloxyethyl]-*N,N*-di-[2-hydroxyethyl]ammonium chloride (1)**: ^{1}H NMR (200 MHz, $CDCl_3$): $\delta = 0.90$ [t, 6H, CH_3-$(CH_2)_5$-], 1.15–1.40 [m, 20H, -$(CH_2)_5$-], 1.45–1.60 [m, 4H, -O-CH_2-CH_2-$(CH_2)_5$-], 3.45 [t, 6H, -O-CH_2-$(CH_2)_6$-], 3.70–3.90 [m, 12H, (HO-CH_2-$CH_2)_2N^+$(CH_2-CH_2-O-)$_2$-], 4.10 [brs, 4H, (HO-CH_2-$CH_2)_2N^+$(CH_2-CH_2-O-)$_2$-]; HRMS (LSIMS): *m*/*z*: calcd for $C_{24}H_{52}NO_4$: 418.3896; found: 418.3913.

***N,N*-Di-[2-*n*-decyloxyethyl]-*N,N*-di-[2-hydroxyethyl]ammonium chloride (2)**: ^{1}H NMR (200 MHz, $CDCl_3$): $\delta = 0.90$ [t, 6H, CH_3-$(CH_2)_7$-], 1.15–1.35 [m, 28H, -$(CH_2)_7$-], 1.45–1.60 [m, 4H, -O-CH_2-CH_2-$(CH_2)_7$-], 3.42 [t, 4H, -O-CH_2-$(CH_2)_8$-], 3.65–3.90 [m, 12H, (HO-CH_2-$CH_2)_2N^+$(CH_2-CH_2-O-)$_2$-], 4.05 [brs, 4H, (HO-CH_2-$CH_2)_2N^+$(CH_2-CH_2-O-)$_2$-]; HRMS (LSIMS): *m*/*z*: calcd for $C_{28}H_{60}NO_4$: 474.4522; found: 474.4526.

***N,N*-Di-[2-*n*-tetradecyloxyethyl]-*N,N*-di-[2-hydroxyethyl]ammonium chloride (4)**: ^{1}H NMR (200 MHz, $CDCl_3$+CD_3OD): $\delta = 0.90$ [t, 6H, CH_3-$(CH_2)_{11}$-], 1.20–1.45 [m, 44H,-$(CH_2)_{11}$-], 1.50–1.65 [m, 4H, -O-CH_2-CH_2-$(CH_2)_{11}$-], 3.45 [t, 4H,-O-CH_2-$(CH_2)_{12}$-], 3.60–3.75 [m, 8H, (HO-CH_2-$CH_2)_2N^+$(CH_2-CH_2-O-)$_2$-], 3.80 [brs, 4H, (HO-CH_2-$CH_2)_2N^+$(CH_2-CH_2-O-)$_2$-], 4.00 [brs, 4H, (HO-CH_2-$CH_2)_2N^+$(CH_2-CH_2-O-)$_2$-]; HRMS (LSIMS): *m*/*z*: calcd for $C_{36}H_{76}NO_4$: 586.5774; found: 586.5798.

***N,N*-Di-[2-*n*-hexadecyloxyethyl]-*N,N*-di-[2-hydroxyethyl]ammonium chloride (5)**: ^{1}H NMR (200 MHz, $CDCl_3$): $\delta = 0.90$ [t, 6H, CH_3-$(CH_2)_{13}$-], 1.15–1.35 [m, 52H, -$(CH_2)_{13}$-], 1.45–1.60 [m, 4H, -O-CH_2-CH_2-$(CH_2)_{13}$-], 3.45 [t, 4H, -O-CH_2-$(CH_2)_{14}$-], 3.60–4.00 [m, 12H, (HO-CH_2-$CH_2)_2N^+$(CH_2-CH_2-O-)$_2$-], 4.10 [brs, 4H, (HO-CH_2-$CH_2)_2N^+$(CH_2-CH_2-O-)$_2$-]; HRMS (LSIMS): *m*/*z*: calcd for $C_{40}H_{84}NO_4$: 642.6400; found: 642.6418.

***N,N*-Di-[2-*n*-octadecyloxyethyl]-*N,N*-di-[2-hydroxyethyl] ammonium chloride (6)**: ^{1}H NMR (200 MHz, $CDCl_3$): $\delta = 0.90$ [t, 6H, CH_3-$(CH_2)_{15}$-], 1.15–1.40 [m, 60H, -$(CH_2)_{15}$-], 1.45–1.65 [m, 4H, -O-CH_2-CH_2-$(CH_2)_{15}$-], 3.42 [t, 4H, -O-CH_2-$(CH_2)_{16}$-], 3.60–3.87 [m, 12H, (HO-CH_2-$CH_2)_2N^+$(CH_2-CH_2-O-)$_2$-], 4.07 [brs, 4H, (HO-CH_2-$CH_2)_2N^+$(CH_2-CH_2-O-)$_2$-]; HRMS (LSIMS): *m*/*z*: calcd for $C_{44}H_{92}NO_4$: 698.7026; found: 698.7050.

All the dihydroxyethyl head group containing DHDEAB analogues **7**–**15** were prepared following the same protocol as outlined in Scheme 2. The necessary starting primary amines **I** were conventionally synthesized in three steps from the corresponding primary alcohols namely, conversion of alcohol to primary azide through the intermediate mesylate followed by reduction of the primary azides with triphenyl phosphine and water. As a representative example, synthetic details for *N,N*-di-*n*-dodecylamine is outlined below.

1-Dodecanal: Pyridinium chlorochromate (2.63 g, 12.3 mmol) and Celite (2.63 g) was taken in dry dichloromethane (13 mL) in a two-necked round-bottomed flask and to this was added *n*-dodecyl alcohol (1.52 g, 8.2 mmol) dissolved in dry dichloromethane (6 mL). The reaction mixture was cooled to 0 °C and stirring was continued at room temperature under nitrogen for 4 h. Dichloromethane was removed on a rotary evaporator. Column chromatographic purification of the residue using 60–120 mesh size silica gel and 10% ethyl acetate in petroleum ether (b.p. 60–80 °C) (*v*/*v*) as the eluent afforded pure title compound as a colorless liquid (1.22 g, 81.5%).

***N,N*-Di-*n*-dodecylamine**: In a 50 mL round-bottomed flask a mixture of *n*-dodecanal (0.28 g, 1.5 mmol), *n*-dodecylamine (0.28 g, 1.5 mmol) was dissolved in dry dichloromethane (10 mL) and the solution was cooled to 0 °C. Anhydrous $MgSO_4$ (0.22 g, 1.8 mmol) was added to the cold solution and the reaction mixture was stirred under N_2 overnight during which period the temperature gradually raised to room temperature. $MgSO_4$ was filtered off, the precipitate washed with methanol (3 × 2 mL) and the combined filtrate was cooled to 0 °C. $NaBH_4$ (0.11 g, 3.0 mmol) was added to the cold solution and the mixture was kept under stirring for 4 h at room temperature. The reaction mixture was then diluted with chloroform (25 mL), washed with water (3 × 25 mL), the chloroform layer dried over anhydrous Na_2SO_4 and filtered. Solvents from the filtrate was removed on a rotary evaporator. Column chromatographic purification of the residue using silica gel 60–120 mesh size and 4% (*v*/*v*) methanol in chloroform as eluent afforded the title secondary amine ($R_f = 0.5$, chloroform/methanol 90:10) as a pale yellowish solid (0.18 g, 33.4%).

***N,N*-Di-*n*-dodecylamine**: ^{1}H NMR (200 MHz, $CDCl_3$): $\delta = 0.8$ [t, 6H, CH_3-$(CH_2)_9$-], 1.05–1.4 [m, 18H, CH_3-$(CH_2)_9$], 1.45–1.7 [m, 4H, NH(CH_2-CH_2-)$_2$-], 2.8 [t, 4H, NH(CH_2-CH_2-)$_2$], 4.0–4.7 [br, N*H*].

***N,N*-Di-*n*-octylamine**: ^{1}H NMR (200 MHz, $CDCl_3$): $\delta = 0.8$ [t, 6H, CH_3-$(CH_2)_5$-], 1.05–1.45 [m, 10H, CH_3-$(CH_2)_5$], 1.6–1.85 [m, 4H, NH(CH_2-CH_2-)$_2$-], 2.8 [t, 4H, NH(CH_2-CH_2-)$_2$], 5.95–6.4 [br, N*H*].

***N,N*-Di-*n*-decylamine**: ^{1}H NMR (200 MHz, $CDCl_3$): $\delta = 0.9$ [t, 6H, CH_3-$(CH_2)_7$-], 1.1–1.45 [m, 14H, CH_3-$(CH_2)_7$], 1.45–1.75 [m, 4H, NH(CH_2-CH_2-)$_2$-], 2.8 [t, 4H, NH(CH_2-CH_2-)$_2$], 4.1–4.7 [br, N*H*].

***N,N*-Di-*n*-tetradecylamine**: ^{1}H NMR (200 MHz, $CDCl_3$): $\delta = 0.9$ [t, 6H, CH_3-$(CH_2)_9$-], 1.15–1.45 [m, 18H, CH_3-$(CH_2)_{11}$], 1.45–1.7 [m, 4H, NH(CH_2-CH_2-)$_2$-], 2.55–2.7 [t, 4H, NH(CH_2-CH_2-)$_2$], 4.0–4.7 [br, N*H*].

***N,N*-Di-*n*-hexadecylamine**: ^{1}H NMR (200 MHz, $CDCl_3$): $\delta = 0.85$ [t, 6H, CH_3-$(CH_2)_{14}$-], 1.15–1.60 [m, 28H, CH_3-$(CH_2)_{14}$], 2.6 [t, 4H, NH(CH_2-CH_2-)$_2$].

***N,N*-Di-*n*-octadecylamine**: ^{1}H NMR (200 MHz, $CDCl_3$): $\delta = 0.85$ [t, 6H, CH_3-$(CH_2)_{15}$-], 1.15–1.35 [m, 30H, CH_3-$(CH_2)_{15}$], 1.4–1.7 [m, 4H, NH(CH_2-CH_2-)$_2$-], 2.6 [t, 4H, NH(CH_2-CH_2-)$_2$].

***N,N*-Oleyl-*n*-octadecylamine**: ^{1}H NMR (200 MHz, $CDCl_3$): $\delta = 0.85$–1.1 [t, 6H, CH_3-$(CH_2)_{15}$-], 1.1–1.5 [m, 18H, CH_3-$(CH_2)_{15}$], 1.6–1.85 [m, 4H, NH(CH_2-CH_2-)$_2$-], 1.95–2.15 [m, 4H, -CH_2-CH=CH-CH_2-], 2.9 [t, 4H, NH(CH_2-CH_2-)$_2$], 5.3–5.6 [t, 2H, -CH_2-CH=CH-CH_2-].

***N,N*-Di-oleylamine**: ^{1}H NMR (200 MHz, $CDCl_3$): $\delta = 0.9$ [t, 6H, CH_3-$(CH_2)_{15}$-], 1.1–1.5 [m, 18H, CH_3-$(CH_2)_{15}$], 1.5–1.75 [m, 4H, NH(CH_2-CH_2-)$_2$-], 2.0 [m, 4H, -CH_2-CH=CH-CH_2-], 2.8 [t, 4H, NH(CH_2-CH_2-)$_2$], 5.3 [t, 2H, -CH_2-CH=CH-CH_2-].

***N,N*-Di-*n*-archidylamine**: ^{1}H NMR (200 MHz, $CDCl_3$): $\delta = 0.9$ [t, 6H, CH_3-$(CH_2)_{17}$-], 1.15–1.6 [m, 34H, CH_3-$(CH_2)_{17}$], 1.6–1.8 [m, 4H, NH(CH_2-CH_2-)$_2$-], 2.95 [t, 4H, NH(CH_2-CH_2-)$_2$], 4.0–4.7 [br, N*H*].

All the new DHDEAB analogues were prepared by quaternizing the appropriate hydrophobic secondary amines with alkaline 2-chloroethanol as outlined in Scheme 2. As a representative example, the details of the final quaternization step for the synthesis of *N,N*-di-*n*-dodecyl-*N,N*-di-*n*-hydroxyethylammonium chloride (amphiphile **9**, Scheme 2) is outlined below.

***N,N*-Di-*n*-dodecyl-*N,N*-dihydroxyethylammonium chloride (9, Scheme 2)**: In a 25 mL round-bottomed flask a mixture of *N,N*-di-*n*-dodecylamine (0.18 g, 0.50 mmol) and 2-chloroethanol (5 mL) was stirred at room temperature for 15 min. NaOH (0.18 g, 0.46 mmol) dissolved in water (1.5 mL) was added and the reaction mixture was heated for 36 h at a temperature of 85 °C. Excess 2-chloroethanol was removed on a rotary evaporator by repeated addition of methanol. Column chromatographic purification of the residue using silica gel (60–120 mesh size) and 10% methanol in chloroform (*v*/*v*) as the eluent afforded the title amphiphile (118.6 mg, 44%) as a colorless liquid ($R_f = 0.4$ 10% methanol in chloroform).

***N,N*-Di-*n*-dodecylammonium chloride (9)**: ^{1}H NMR (200 MHz, $CDCl_3$): $\delta = 0.9$ [t, 6H, CH_3-$(CH_2)_n$-], 1.55–1.9 [m, 4H, ($HOCH_2$-$CH_2)_2N$(CH_2-CH_2)$_2$-], 3.3–3.5 [m, 4H, ($HOCH_2$-$CH_2)_2N$(CH_2-$(CH_2)_2$], 3.55–3.85 [m, 4H, ($HOCH_2$-$CH_2)_2N$(CH_2-$CH_2)_2$-], 3.95–4.2 [m, 4H, ($HOCH_2$-$CH_2)_2N^+$(CH_2-CH_2.)$_2$], 5.20–5.45 [m, 2H, O*H*]; FABMS (LSIMS): *m*/*z*: 442 [*M*+H]$^+$ for $C_{28}H_{60}NO_2$; HRMS(LSIMS): *m*/*z*: calcd for $C_{28}H_{60}NO_2$: 442.4624; found: 442.4610.

***N,N*-Di-*n*-octyl-*N,N*-dihydroxyethylammonium chloride (7)**: ^{1}H NMR (200 MHz, $CDCl_3$): $\delta = 0.9$ [t, 6H, (CH_3-$CH_2)_n$-], 1.15–1.45 [m, 20H, -$(CH_2)_5$-], 1.5–1.8 [m, 4H, ($HOCH_2$-$CH_2)_2N^+$(CH_2-CH_2-)$_2$], 3.3–3.5 [m, 4H, (HO-CH_2-$CH_2)_2N^+$(CH_2-CH_2-)$_2$], 3.50–3.75 [m, 4H, ($HOCH_2$-$CH_2)_2N^+$(CH_2-CH_2-)$_2$], 3.95–4.15 [m, 4H, ($HOCH_2$-$CH_2)_2N^+$(CH_2-CH_2-)$_2$]; FABMS(LSIMS): *m*/*z*: 330 for $C_{20}H_{42}NO_2$; HRMS(LSIMS): *m*/*z*: calcd for $C_{20}H_{42}NO_2$: 330.3372; found: 330.3358.

***N,N*-Di-*n*-decyl-*N,N*-dihydroxyethylammonium chloride (8)**: ^{1}H NMR (200 MHz, $CDCl_3$): $\delta = 0.9$ [t, 6H, CH_3-$(CH_2)_n$-], 1.20–1.45 [m, 28H, -$(CH_2)_7$-], 1.55–1.88 [m, 4H, $(HOCH_2$-$CH_2)_2N^+(CH_2$-CH_2-$)_2$], 3.3–3.5 [m, 4H, $(HOCH_2$-$CH_2)_2N^+(CH_2$-CH_2-$)_2$], 3.50–3.8 [m, 4H, $(HOCH_2$-$CH_2)_2N^+(CH_2$-$CH_2)_2$], 3.95–4.15 [m, 4H, $(HOCH_2$-$CH_2)_2N^+(CH_2$-CH_2-$)_2$]; FABMS(LSIMS): *m/z*: 386 for $C_{24}H_{52}NO_2$; HRMS(LSIMS): *m/z*: calcd for $C_{24}H_{52}NO_2$: 386.3998; found: 386.4002.

***N,N*-Di-*n*-tetradecylammonium chloride (10)**: (200 MHz, $CDCl_3$): $\delta = 0.9$ [t, 6H, CH_3-$(CH_2)_n$-], 1.20–1.5 [m, 44H, -$(CH_2)_{11}$-], 1.55–1.9 [m, 4H, $(HOCH_2$-$CH_2)_2N^+(CH_2$-CH_2-$)_2$], 3.3–3.5 [m, 4H, $(OHCH_2$-$CH_2)_2N^+(CH_2$-CH_2-$)_2$], 3.55–3.85 [m, 4H, $(OHCH_2$-$CH_2)_2N^+(CH_2$-CH_2-$)_2$], 3.95–4.2 [m, 4H, $(OHCH_2$-$CH_2)_2N^+(CH_2$-CH_2-$)_2$], 5.20–5.45 [m, 2H, -O*H*]; FABMS (LSIMS): *m/z*: 498 $[M+H]^+$ for $C_{32}H_{68}NO_2$; HRMS(LSIMS): *m/z*: calcd for $C_{32}H_{68}NO_2$: 498.5250; found: 498.5274.

***N,N*-Di-*n*-hexadecyldihydroxyethylammonium chloride (11)**: ^{1}H NMR (200 MHz, $CDCl_3$): $\delta = 0.9$ [t, 6H, $(CH_3$-$CH_2)_n$-], 1.20–1.5 [m, 52H, -$(CH_2)_{13}$-], 1.55–1.85 [m, 4H, $(HOCH_2$-$CH_2)_2N^+(CH_2$-CH_2-$)_2$], 3.35–3.6 [m, 4H, $(HOCH_2$-CH_2-$)_2N^+(CH_2$-CH_2-$)_2$], 3.60–3.80 [m, 4H, $(HOCH_2$-$CH_2)_2N^+(CH_2$-CH_2-$)_2$], 3.95–4.2 [m, 4H, $(HOCH_2$-$CH_2)_2N^+(CH_2$-CH_2-$)_2$]; FABMS (LSIMS): *m/z*: 555 $[M+H]^+$ for $C_{36}H_{76}NO_2$.

***N,N*-Di-*n*-octadecyl-*N,N*-dihydroxyethylammonium chloride (12)**: ^{1}H NMR (200 MHz, $CDCl_3$): $\delta = 0.9$ [t, H, CH_3-$(CH_2)_n$-], 1.2–1.4 [m, 60H, -$(CH_2)_{15}$-], 1.6–1.85 [m, 4H, $(HOCH_2$-$CH_2)_2N^+(CH_2$-CH_2-$)_2$], 3.3–3.5 [m, 4H, $(HOCH_2$-$CH_2)_2N^+(CH_2$-CH_2-$)_2$], 3.6 [m, 4H, $HOCH_2$-$CH_2)_2N^+(CH_2$-CH_2-$)_2$], 4.0–4.1 [m, 4H, $(HOCH_2$-$CH_2)_2N^+(CH_2$-CH_2-$)_2$], 5.2 [m, 2H, O*H*]; FABMS (LSIMS): *m/z*: 611 $[M+H]^+$ for $C_{40}H_{84}NO_2$; HRMS(LSIMS): *m/z*: calcd for $C_{40}H_{84}NO_2$: 610.6502; found: 610.6525.

***N*-Oleyl-*n*-octadecyl-*N,N*-dihydroxyethylammonium chloride (13)**: ^{1}H NMR (200 MHz, $CDCl_3$): $\delta = 0.9$ [t, 6H, CH_3-$(CH_2)_n$], 1.20–1.45 [m, 52H, -$(CH_2)_{13}$-], 1.6–1.8 [br, 4H, $(HOCH_2$-$CH_2)_2N^+(CH_2$-CH_2-$)_2$], 1.90–2.10 (m, -CH_2-CH=CH-CH_2-); 3.3–3.5 [m, 4H, $(HOCH_2$-$CH_2)_2N^+(CH_2$-CH_2-$)_2$], 3.55–3.8 [m, 4H, $(HO$-CH_2-$CH_2)_2N^+(CH_2$-CH_2-$)_2$], 3.95–4.15 [m, 4H, $(HOCH_2$-$CH_2)_2N^+(CH_2$-CH_2-$)_2$], 5.28–5.4 [m, 2H, -CH_2-C*H*=C*H*-CH_2-], 5.45–5.55 [br, 2H, O*H*]; FABMS(LSIMS): *m/z*: 609 $[M+H]^+$ for $C_{40}H_{82}NO_2$; HRMS(LSIMS): *m/z*: calcd for $C_{40}H_{82}NO_2$: 608.6346; found: 608.6354.

***N,N*-Di-*n*-oleyl-*N,N*-dihydroxyethylammonium chloride (14)**: ^{1}H NMR (200 MHz, $CDCl_3$): $\delta = 0.9$ [t, 6H, CH_3-$(CH_2)_n$], 1.20–1.5 [m, 44H, (-CH_2-$(CH_2)_5$-CH_2-CH=CH-CH_2-$(CH_2)_6$-$CH_3)_2$], 1.60–1.80 [br, 4H, $CH_3(HOCH_2$-$CH_2)N^+(CH_2$-CH_2-$)_2$], 1.90–2.10 [m, 8H, (-CH_2-CH=CH-CH_2-$)_2$], 3.3–3.5 [m, 4H, $(HOCH_2$-$CH_2)_2N^+(CH_2$-CH_2-$)_2$], 3.5–3.7 [m, 4H, $(HO$-CH_2-$CH_2)_2N^+(CH_2$-CH_2-$)_2$], 3.95–4.15 [m, 4H, $(HOCH_2$-$CH_2)_2N^+(CH_2$-CH_2-$)_2$], 5.3 [m, 4H, -(-CH_2C*H*=C*H*-CH_2-)$_2$]; FABMS (LSIMS): *m/z*: 607 $[M+H]^+$ for $C_{40}H_{80}NO_2$.

***N,N*-Di-*n*-arachidyl-*N,N*-dihydroxyethylammonium chloride (15)**: ^{1}H NMR (200 MHz,$CDCl_3$): $\delta = 0.9$ [t, 6H, CH_3-$(CH_2)_n$-], 1.2–1.4 [m, 68H,-$(CH_2)_{34}$-], 1.45–1.65 [m, 4H, $(HOCH_2$-$CH_2)_2N^+(CH_2$-$CH_2)_2$], 3.33.5 [m, 4H, $(HOCH_2$-$CH_2)_2N^+(CH_2$-CH_2-$)_2$], 3.53–3.65 [m, 4H $(HOCH_2CH_2)_2N^+(CH_2CH_2)_2$], 3.95–4.15 [m, 4H, $(HOCH_2$-$CH_2)_2N^+(CH_2$-CH_2-$)_2$]; FABMS (LSIMS): *m/z*: 667 $[M+H]^+$ for $C_{44}H_{92}NO_2$.

Preparation of liposomes and plasmid DNA: Preparation of liposomes, isolation of DNA and characterizaton of DNA were done, essentially, as described in our previous work.[5] Briefly, cationic amphiphiles and cholesterol were co-dried in chloroform under nitrogen gas and hydrated in sterile water overnight. The vortexed liposomes were sonicated to clarity. pCMV β-gal plasmid DNA was prepared by alkaline lysis procedure and purified by PEG-8000 precipitation according to the published procedures.[31] The plasmid preparations showing a value of A_{260}/A_{280} more than 1.8 were used.

Transfection of cells: Transfection of the cells were done essentially as described earlier.[5] Briefly, COS-1 or CHO cells were seeded at a density of 15000 cells per well in a 96-well plate eighteen hours before the transfection. 0.3 μg of plasmid was complexed with varying amount of lipid and cholesterol (0.05–4.3 nmol) in plain DMEM medium for 30 min. The charge ratios were varied from 0.1:1 to 9:1 (+/−) over this range of the lipid. The complex was diluted to 100 μL with plain DMEM and added to the wells. After 3 h of incubation, 100 μL of DMEM with 10% FCS was added to the cells. The medium was changed to 10% complete medium after 24 h and the reporter gene activity was assayed after 48 h. Washed cells were lysed in 50 μL of lysis buffer (0.25 M Tris·HCl, pH 8.0 and 0.5% NP40). The β-galactosidase activity per well was estimated by adding 50 μL of 2× substrate solution (1.33 mg mL^{-1} ONPG, 0.2 M sodium phosphate, pH 7.15 and 2 mM magnesium chloride) to the lysate in a 96-well plate. Absorption at 405 nm was converted to β-galactosidase units by using calibration curve constructed with pure commercial β-galactosidase enzyme. The values of β-galactosidase units in replicate plates assayed on the same day varied by less than 30%. The transfection efficiency values are the average values from four replicate transfection plates assayed on the same day. Each transfection experiment was repeated three times on different days and the day-to-day variation in average transfection efficiency was found to vary within 20–30%. The transfection profiles obtained on different days were identical.

Dynamic light scattering measurements: Dynamic light scattering (DLS) measurements were performed using a DLS-700 instrument from Otsuka Electronics Co. Ltd., Japan, fitted with a 5 mW He/Ne laser operating at 632.8 nm by placing the sample tube in the thermostated chamber of the goniometer. All measurements were taken at 90° angle. Each sample was prepared using doubly distilled water filtered several times through a Millipore 0.22 μm membrane filter. The DLS intensity data were processed using the instrumental software to obtain the hydrodynamic diameter (d_h).

Exclusion of ethidium bromide (EtBr) from DNA by the cationic lipids: The extent of EtBr binding to the DNA was monitored by the changes in the fluorescence. EtBr fluorescence was monitored in Hitachi 4500 fluorimeter by setting the excitation wavelength at 518 nm and emission wavelength at 585 nm. To 1 mL TE buffer (pH 8.0), 0.78 nmol DNA and 2.5 nmol EtBr were added. The change in fluorescence was monitored after adding small volumes of lipids **1**–**15** to the EtBr/DNA complex. Arbitrary fluorescence values were recorded after allowing sufficient time for equilibration. The order of addition of EtBr or lipid to DNA did not alter the final values indicating that the equilibrium does not depend on the order of addition and reaches in minutes. Percent fluorescence was calculated considering the fluorescence value in the absence of lipid as 100.

Toxicity assay: Cytotoxicity of lipids **1**–**15** was assessed using 3-(4,5-dimethylthiazol-2-yl)-2,5-diphenyltetrazolium bromide (MTT) reduction assay as described earlier.[32] The cytotoxicity assay was performed in 96-well plates by maintaining the ratio of number of cells to amount of cationic lipid constant as in transfection experiments. MTT was added three hours after adding the cationic lipid to the cells.

Anisotropy measurements of cationic liposomes: Cationic lipids were dissolved in chloroform along with DPH at a mol ratio of 300:1 and dried under N_2 gas. The lipid was hydrated in buffer (TrisCl, pH 7.4, 100 mM) for few hours and then sonicated in a Branson (Model B-50) sonifier at temperatures above the transition temperatures till clarity. Anisotropy was calculated by recording the fluorescence values (excitation at 354 nm; emission at 427 nm) at parallel and perpendicular polariser positions in an Hitachi F4010 fluorimeter. Anisotropy was calculated according to the procedure given in Shinitzky and Barenholz (M. Shinitzky, Y. Barenholz, *Biochem. Biophys. Acta* **1978**, *515*, 367–394).

Acknowledgement

Financial support for this work from the Department of Biotechnology, New Delhi, Government of India (to A.C.) is gratefully acknowledged. Financial supports in the form of doctoral research fellowships from the Council of Scientific and Industrial Research (CSIR), Government of India, New Delhi (to R.S.S. and R.B.) and University Grant Commision (UGC), Government of India, New Delhi (to K.M. and S.K.H.) are gratefully acknowledged.

[1] S. Li, L. Huang, *Gene Ther.* **2000**, *7*, 31–34.
[2] D. Luo, W. M. Saltzman, *Nat. Biotechnol.* **2000**, *18*, 33–37.
[3] A. D. Miller, *Angew. Chem.* **1998**, *110*, 1862–1880; *Angew. Chem. Int. Ed.* **1998**, *37*, 1768–1785 and references therein.
[4] S. Kawakami, A. Sato, M. Nishikawa, F. Yamashita, M. Hashida, *Gene Ther.* **2000**, *7*, 292–299.
[5] R. Banerjee, P. K. Das, G. V. Srilakshmi, A. Chaudhuri, N. M. Rao, *J. Med. Chem.* **1999**, *42*, 4292–4299.

  0947-6539/02/0804-0908 $ 17.50+.50/0 *Chem. Eur. J.* **2002**, *8*, No. 4

[6] J. P. Behr, B. Demeneix, J. P. Loeffler, J. Perez-Mutul, *Proc. Natl. Acad. Sci. USA* **1989**, *86*, 6982–6986.
[7] J. Wang, X. Guo, Y. Xu, L. Barron, F. C. Szoka, Jr., *J. Med. Chem.* **1998**, *41*, 2207–2215.
[8] G. Byk, C. Dubertret, V. Escriou, M. Frederic, G. Jaslin, R. Rangara, B. Pitard, J. Crouzet, P. Wils, B. Schwartz, D. Scherman, *J. Med. Chem.* **1998**, *41*, 224–235.
[9] G. Byk, B. Wetzer, M. Frederic, C. Dubertret, B. Pitard, G. Jaslin, D. Scherman, *J. Med. Chem*. **2000**, *43*, 4377–4387.
[10] M. J.Bennett, A. M. Aberle, R. P. Balasubramaniam, J. G. Malone, R. W. Malone, M. H. Nantz, *J. Med. Chem.* **1997**, *40*, 4069–4078.
[11] V. Floch, G. Le Bolc'h, C. Gable-Guillaume, N. Le Bris, J.-J. Yaouanc, H. des Abbayes, C. Férec, J.-C. Clément, *Eur. J. Med. Chem.* **1998**, *41*, 923–934.
[12] J. P. Behr, *Acc. Chem. Res.* **1993**, *26*, 274–278.
[13] D. M. Lynn, R. Langer, *J. Am. Chem. Soc.* **2000**, *122*, 10761–10768.
[14] Y. Liu, L. C. Mounkes, H. D. Liggitt, C. S. Brown, I. Solodin, T. D. Heath, R. J. Debs, *Nat. Biotechnol.* **1997**, *15*, 167–173.
[15] N. S. Templeton, D. D. Lasic, P. M. Frederik, H. H. Strey, D. D. Roberts, G. N. Pavlakis, *Nat. Biotechnol.* **1997**, *15*, 647–652.
[16] N. J. Caplen, E. W. Alton, P. G. Middleton, J. R. Dorin, B. J. Stevenson, X. Gao, S. R. Durham, P. K. Jeffery, M. E. Hodson, C. Coutelle, L. Huang, D. J. Porteous, R. Williamson, D. M. Geddes, *Nat. Med.* **1995**, *1*, 39–46.
[17] E. Guénin, A.-C. Hervé, V. Floch, S. Loisel, J.-J. Yaouanc, J.-C. Clément, C. Férec, H. des Abbayes, *Angew. Chem.* **2000**, *112*, 643–645; *Angew. Chem. Int. Ed.* **2000**, *39*, 629–631.
[18] R. G. Cooper, C. J. Etheridge, L. Stewart, J. Marshall, S. Rudginsky, S. H. Cheng, A. D. Miller, *Chem. Eur. J.* **1998**, *4*, 137–154.
[19] C. J. Wheeler, P. L. Felgner, Y. J. Tsai, J. Marshall, L. Sukhu, G. Doh, J. Hartikka, J. Nietupski, M. Manthorpe, M. Nichols, M. Piewe, X. Liang, J. Norman, A. Smith, S. H. Cheng, *Proc. Natl. Acad. Sci. USA* **1996**, *93*, 11454–11459.
[20] I. Solodin, C. Brown, M. Bruno, C. Chow, E.-H. Jang, R. Debs, T. A. Heath, *Biochemistry* **1995**, *34*, 13537–13544.
[21] Y. Liu, D. Liggitt, G. Tu, W. Zhong, K. Gaensler, R. Debs, *J. Biol. Chem.* **1995**, *270*, 24864–24870.
[22] J. H. Felgner, R. Kumar, C. N. Sridhar, C. J. Wheeler, Y.-J. Tsai, R. Border, P. Ramsey, M. Martin, P. L. Felgner, *J. Biol. Chem.* **1994**, *269*, 2550–2561.
[23] E. W. Alton, P. G. Middleton, N. J. Caplen, S. N. Smith, D. M. Steel, F. M. Munkonge, P. K. Jeffery, B. J. Stevension, G. McLachlan, J. R. Dorin, D. J. Porteous, *Nat. Genet.* **1993**, *5*, 135–142.
[24] M. A. W. Eaton, T. S. Baker, C. F. Catterall, K. Crook, G. S. Macaulay, B. Mason, T. J. Norman, D. Parker, J. J. B. Perry, R, J. Taylor, A. Turner, A. N. Weir, *Angew. Chem.* **2000**, *112*, 4229–4233; *Angew. Chem. Int. Ed.* **2000**, *39*, 4063–4067.
[25] X. Gao, L. Huang, *Biochem. Biophys. Res. Commun.* **1991**, *179*, 280–285.
[26] P. L. Felgner, T. R. Gadek, M. Holm, R. Roman, W. Chan, M. Wenz, J. P. Northorp, G. M. Ringold, M. Danielsen, *Proc. Natl. Acad. Sci. USA* **1987**, *84*, 7413–7417.
[27] Y. K. Ghosh, S. S. Visweswarial, S. Bhattacharya, *FEBS Lett.* **2000**, *473*, 341–344.
[28] T. Fichert, A. Regelin, U. Massing, *Bioorg. Med. Chem. Lett.* **2000**, *10*, 787–791.
[29] A. E. Regelin, S. Fankhaenel, L. Gurtesch, C. Prinz, G. v. Kiedrowski, U. Massing, *Biochim. Biophys. Acta* **2000**, *1464*, 151–164.
[30] T. Ren, Y. K. Song, G. Zhang, D. Liu, *Gene Ther.* **2000**, *7*, 764–768.
[31] J. Sambrook, E. F. Fritsch, T. Maniatis, *Molecular Cloning*: *A Laboratory Manual*, 2nd ed., Cold Spring Harbor Laboratory Press, Cold Spring Harbor, NY, **1989**.
[32] M.-B. Hansen, S. E. Neilson, K. Berg, *J. Immunol. Methods* **1989**, *119*, 203–210.

Received: May 22, 2001
Revised: September 10, 2001 [F3277]